

IS DOUBLE REIONIZATION PHYSICALLY PLAUSIBLE?

STEVEN R. FURLANETTO¹ & ABRAHAM LOEB²

Draft version May 23, 2019

ABSTRACT

Recent observations of $z \sim 6$ quasars and the cosmic microwave background imply a complex history to cosmic reionization. Such a history requires some form of feedback to extend reionization over a long time interval, but the nature of the feedback and how rapidly it operates remain highly uncertain. Here we focus on one aspect of this complexity: *which physical processes can cause the global ionized fraction to evolve non-monotonically with cosmic time?* We first examine how galactic winds affect the transition from metal-free to normal star formation. Because winds expand much more slowly than ionization fronts, we find that this mechanism cannot be responsible for double reionization given plausible parameters for the winds. We next consider photoheating, which causes the cosmological Jeans mass to increase in ionized regions and hence suppresses galaxy formation there. Double reionization is more plausible in this case, but only if small halos form stars efficiently and if the suppression from photoheating is strong relative to current expectations. Finally, we consider H₂ photodissociation, in which the buildup of a soft UV background suppresses star formation in small halos. This too can cause the ionized fraction to temporarily decrease, but only during the earliest stages of reionization. For all of these mechanisms, double reionization appears less likely than a long, but still monotonic, ionization history. Finally, we briefly consider the effects of some of these feedback mechanisms on the topology of reionization.

Subject headings: cosmology: theory – galaxies: evolution – intergalactic medium

1. INTRODUCTION

The epoch of reionization marks the time when collapsed objects began to influence the diffuse intergalactic medium (IGM) and first rendered it transparent to ultraviolet photons. It is an important milestone signaling the end of the “cosmological dark ages” and the emergence of the first luminous sources in the universe. A wide variety of observational probes have been used recently to constrain not only the reionization process itself but also the properties of the sources driving it.

The most powerful observational constraints come from Ly α absorption spectra of high redshift quasars (Becker et al. 2001; Fan et al. 2002; White et al. 2003). All known quasars with $z > 6$ show a complete Gunn & Peterson (1965) trough as well as a rapidly evolving neutral fraction indicative of the final stages of reionization (though see Songaila 2004 for a different interpretation). This conclusion is strengthened by analyses of the proximity effects around these quasars (Wyithe & Loeb 2004a; Mesinger & Haiman 2004). The second clue is from measurements of the large scale polarization anisotropies of the the cosmic microwave background (CMB), which imply a high optical depth to electron scattering and require reionization to begin at $z \gtrsim 14$ (Kogut et al. 2003; Spergel et al. 2003). A third clue comes from the temperature of the Ly α forest at $z \sim 3$, which is relatively high and indicates that the neutral fraction changed substantially at $z \lesssim 10$ (Theuns et al. 2002; Hui & Haiman 2003).

Taken together, these constraints imply a complex and extended reionization history, inconsistent with a simple scenario involving a single type of source: in that case reionization should have been rapid and monotonic (because structure

formation proceeds hierarchically and accelerates throughout the era of interest; see Barkana & Loeb 2001 and references therein). Extending reionization over a longer interval requires the properties of the sources to evolve in some way. Such a change could occur naturally due to the feedback of stars on their environment, because the first galaxies form out of metal-free gas and have exceedingly shallow gravitational potential wells. A number of models have been developed to reconcile the disparate inferences about reionization (Wyithe & Loeb 2003a,b; Cen 2003a,b; Haiman & Holder 2003; Sokasian et al. 2004; Fukugita & Kawasaki 2003; Somerville & Livio 2003; Onken & Miralda-Escudé 2004), all incorporating some sort of feedback mechanism to decrease the ionizing efficiency of the sources. The resulting ionization histories display a wide range of features and can extend over long redshift intervals. One of the more intriguing possibilities is so-called *double reionization*. We will use this term to designate histories in which the global ionized fraction \bar{x}_i decreases with cosmic time over some interval. Such models provide the clearest signatures of feedback and should be the easiest to observe with future 21 cm tomography measurements (Furlanetto et al. 2004c). They can be contrasted with “stalling” models in which \bar{x}_i increases monotonically but the feedback mechanism still shapes the overall evolution.

In this paper, we will critically examine the plausibility of the physical processes that may lead to double reionization. Existing models attribute double reionization to three different feedback mechanisms. The first is the transition from metal-free Population III (hereafter Pop III) star formation to “normal” Population II (hereafter Pop II) star formation as observed in the local universe. If Pop III stars are massive, they can produce approximately an order of magnitude more ionizing photons per baryon than do normal stars (Bromm et al. 2001b). The first stars therefore efficiently ionized the IGM; however, as Pop III stars died and exploded, they expelled metals and enriched the IGM. Once star-forming regions reached a typical metallicity of $Z \sim 10^{-3.5} Z_\odot$, the excess

¹ Division of Physics, Mathematics, & Astronomy; California Institute of Technology; Mail Code 130-33; Pasadena, CA 91125; sfurlane@tapir.caltech.edu

² Harvard-Smithsonian Center for Astrophysics, 60 Garden Street, Cambridge, MA 02138; aloe@cfa.harvard.edu

cooling provided by the metals could reduce the Jeans mass and switch the star-formation mode from Pop III to Pop II (Bromm et al. 2001a; Bromm & Loeb 2003), thus lowering the ionizing efficiency. Under some circumstances, Pop II stars could no longer counteract recombinations and so \bar{x}_i would decrease. Unfortunately, existing models have treated this transition crudely. Both Cen (2003a) and Wyithe & Loeb (2003a) assigned a single, universal redshift at which star formation switches between the two modes; the redshift was taken to be the time when the mean metallicity of the universe passed the above threshold. Both found that double reionization occurred for a range of input parameters. However, different regions of the universe are expected to reach the same evolutionary stage of structure formation at different cosmic times due to modulation by inhomogeneities on large scales; this cosmic variance is particularly large at high redshifts (Barkana & Loeb 2004). Haiman & Holder (2003) pointed out that if the Pop III/Pop II transition is spread over a similarly long time interval, double reionization no longer occurs. However, they did not calculate the plausible duration of the transition, and they conflated the metallicity transition with a change in the mass threshold of galaxy halos for star formation. In this paper, we will explicitly compute when and how rapidly the Pop III/Pop II transition occurs using a physical model for enrichment by galactic winds. Like Scannapieco et al. (2003), we find that the transition must occur over an extended redshift interval and only after reionization is complete. In such a scenario, double reionization requires a number of unlikely assumptions. We will begin in §2 by estimating the fraction of collapsing material able to form pristine objects in the absence of galactic winds. We then develop a simple model for wind enrichment in §3 and show how the different enrichment scenarios affect the global reionization history in §4.

A second feedback mechanism is photoheating. Reionization raises the IGM temperature from $T \lesssim 100$ K to $T \gtrsim 10^4$ K, increasing the ambient pressure and hence the cosmological Jeans mass (Rees 1986; Efstathiou 1992). As a result, low-mass halos can no longer collapse in ionized regions and the star formation rate decreases sharply. The degree of suppression is not clear. Early work suggested that this mechanism prevents halos with circular velocities $V_c \lesssim 30\text{--}50$ km s⁻¹ from forming (Thoul & Weinberg 1996; Kitayama & Ikeuchi 2000). However, Dijkstra et al. (2004a) have shown that the suppression is considerably weaker near the time of reionization, because in that case many halos have already begun to collapse and their high densities shield them from the ionizing background. At the same time, existing halos with virial temperatures $T_{\text{vir}} \lesssim 10^4$ K will photoevaporate as they absorb ionizing photons (Barkana & Loeb 1999; Shapiro et al. 2004). The net effect is that, as reionization proceeds, the mass threshold for galaxy formation increases by some (uncertain) amount and reionization slows down. Again, in such a situation it is possible for the ionizing sources to “overshoot” and for recombinations to dominate for a time. This mechanism has been included in most existing models and rarely been found to produce double reionization. Nevertheless, there has been no systematic study of the requirements for such a phase. In §5, we show that photoheating *can* cause double reionization, but only in limited circumstances. We will argue that many existing models underestimate the speed of the transition and hence artificially suppress double reionization.

A third and final feedback mechanism is the photo-

dissociation of H₂. Rotational transitions of H₂ provide a cooling channel that operates in halos with $T_{\text{vir}} \gtrsim 200$ K (Haiman et al. 1996; Tegmark et al. 1997), well below the threshold at which atomic cooling becomes efficient. The first halos to form stars in any hierarchical model have a low mass and therefore rely on H₂ for their cooling (Abel et al. 2002; Bromm et al. 2002). However, H₂ is fragile and is easily dissociated by soft UV photons in the Lyman-Werner band (11.26–13.6 eV) (Haiman et al. 1997). Once the first stars build up a sufficient UV background, this cooling channel terminates and the minimum halo mass to form stars increases; operationally this mechanism is similar to photoheating although it operates at a lower halo mass scale. We will consider whether this scenario can lead to double reionization in §5.1.

Of course, by suppressing the ionizing efficiency in biased regions these feedback mechanisms affect not only the global reionization history but also its topology. As recently stressed by Furlanetto et al. (2004b, hereafter FZH04), the topology of reionization is observable through 21 cm tomography (see also Furlanetto et al. 2004c) and through Ly α absorption (Furlanetto et al. 2004a; Wyithe & Loeb 2004b). Although a much more difficult problem to approach analytically than the global evolution, it is also worth considering what signatures one might expect to see in the bubble size distribution from these feedback mechanisms. We briefly consider this question in §6 and then discuss other consequences of our results in §7.

Throughout our discussion we assume a cosmology with $\Omega_m = 0.3$, $\Omega_\Lambda = 0.7$, $\Omega_b = 0.046$, $H_0 = 100h$ km s⁻¹ Mpc⁻¹ (with $h = 0.7$), $n = 1$, and $\sigma_8 = 0.9$, consistent with the most recent measurements (Spergel et al. 2003). We will use comoving units unless otherwise specified.

2. THE FORMATION RATE OF NEW HALOS

In order to compute the properties of the Pop III/Pop II transition, we must examine how galaxies form and grow. We divide newly-collapsed gas (i.e., baryons that have just been incorporated into galaxies able to form stars) into two components. First, some fraction of the gas accretes onto existing halos that have already formed stars. Provided that the cumulative star formation efficiency f_* in an existing halo was sufficiently large to enrich itself and the accreting material beyond the threshold metallicity Z_t for forming Pop II stars, this component of newly collapsing gas will not make Pop III stars (assuming that metals are efficiently mixed within galaxies). The metallicity threshold is thought to be $Z_t \sim 10^{-3.5} Z_\odot$ (Bromm et al. 2001a; Bromm & Loeb 2003), which requires $f_* \gtrsim 10^{-5} (0.5/f_Z) (Z_t/10^{-3.5} Z_\odot)$, where f_Z is the fraction of the stellar mass converted into heavy elements. Heger & Woosley (2002) find $f_Z \sim 0.5$ for stars which undergo pair-instability supernovae, although not all massive stars actually explode so this is only an upper limit to the true value. The fraction is somewhat smaller (but still $\gtrsim 0.1$) for normal initial mass functions (IMFs). The metallicity threshold for Pop II star formation is sufficiently small that we expect *any* halo that has previously form stars to make only Pop II stars after the initial starburst. There is one caveat to this assumption: if the metals remain highly clumped in the halo, it may still be possible to form Pop III stars in pristine uncontaminated subclumps. Since this would only slow down the transition between the two star formation modes, and we subsequently demonstrate that double reionization is difficult to achieve, we will conservatively ignore this possibility.

To form Pop III stars, gas must therefore collapse into a “new” or “fresh” halo that is just now able to form stars for the first time. We take this criterion to be a minimum galaxy mass m_{\min} determined by the physics of radiative cooling. We will typically assume m_{\min} corresponds to $T_{\text{vir}} = 10^4$ K, the threshold temperature above which atomic hydrogen cooling is effective (e.g., Barkana & Loeb 2001). Thus, to find the *maximal* rate at which Pop III stars can form, we wish to know the rate at which halos of mass $m \approx m_{\min}$ form.

2.1. A Simple Model

In principle, this is a well-defined problem. Given the comoving number density of halos per unit mass as a function of redshift, $n(m, z)$, and the rate at which these halos merge per unit volume, $n(m_1, z) n(m_2, z) Q(m_1, m_2, z)$, we can compute the rate at which of halos merge to form new objects with masses above m_{\min} . Unfortunately, as recently emphasized by Benson et al. (2004), the merger rates typically used in cosmological studies (Bond et al. 1991; Lacey & Cole 1993) are not well-defined. The problem is most easily seen by noting that $Q(m_1, m_2) \neq Q(m_2, m_1)$ in the extended Press-Schechter (EPS) formalism. The fundamental problem is that this formalism does not assign points in space to unique halos: the smoothing procedure implicit in these approaches requires that neighboring points be identified with halos of different masses, even though they must physically be part of the same object. Merger rates, which by definition require the mass to be assigned to halos, are thus ill-defined quantities. As a consequence, merger tree algorithms based on the EPS formalism either do not reproduce the proper mass function or do not conserve mass during the individual time steps, although ad hoc procedures to alleviate these problems have been developed (e.g., Somerville & Kolatt 1999).

We will therefore take a simpler approach (Sasaki 1994; Verde et al. 2001). Given the Press & Schechter (1974) mass function, we can compute the total rate of change of the halo mass function:

$$\frac{dn(m)}{dz} = n(m) \left| \frac{d\nu}{dz} \right| \left(\nu - \frac{1}{\nu} \right), \quad (1)$$

where $\nu = \delta_c(z)/\sigma(m)$, $\delta_c(z)$ is the critical density for collapse, and $\sigma^2(m)$ is the variance of the density field smoothed on the mass scale m . Of course, this is not equal to the creation rate of halos of a given mass; rather, it is the difference between the creation rate and the destruction rate. However, the two terms in the derivative can be conveniently identified as creation and destruction terms. For rare, massive halos (with $\nu \gg 1$), the creation term should dominate because there are only a small number of larger objects into which the halo can be absorbed. The creation rate should therefore increase with increasing ν . Halos with $\nu \ll 1$, on the other hand, are already common. As the nonlinear mass scale rises, these small halos must accrete onto more massive objects. Thus we expect the destruction term to increase with decreasing ν . The two terms in equation (1) have the correct limiting behavior, although of course the split does not capture all of the physics, particularly when $\nu \sim 1$. Nevertheless, we will take this simple prescription as our fiducial model because there is no other self-consistent treatment for the creation rate. Noting that the only halos that can form from two progenitors with $m < m_{\min}$ have final masses in the range $m_{\min} \leq m \leq 2m_{\min}$, the rate at which genuinely new halos form is approximately

$$\frac{df_{\text{new}}}{dz} \approx \left(\frac{m_{\min}^2}{\bar{\rho}} \right) \nu n(m) \left| \frac{d\nu}{dz} \right|, \quad (2)$$

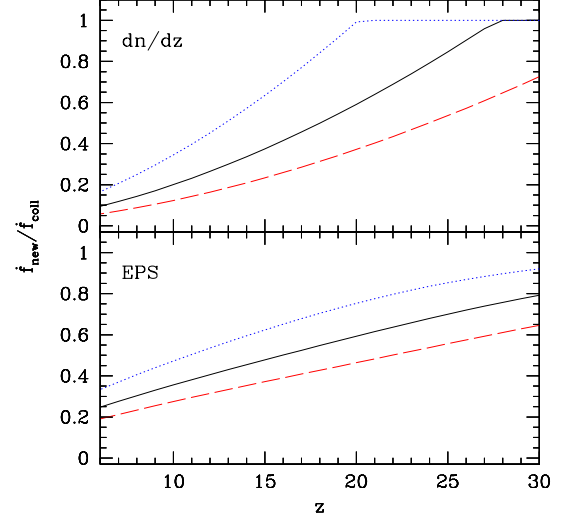


FIG. 1.— Evolution of the fraction of gas collapsing into new halos. *Top:* Approximate model based on eq. (2). *Bottom:* EPS model. In each panel, the solid lines have our default m_{\min} (corresponding to $T_{\text{vir}} = 10^4$ K). The dashed and dotted curves correspond to a decrease or an increase m_{\min} by an order of magnitude.

where $\bar{\rho}$ is the mean cosmic density.

The top panel of Figure 1 shows the evolution of df_{new}/dz relative to the total rate of collapse df_{coll}/dz , where

$$f_{\text{coll}} = \text{erfc} \left[\frac{\delta_c(z)}{\sqrt{2}\sigma_{\min}} \right] \quad (3)$$

is the fraction of matter bound to halos with $m > m_{\min}$ and $\sigma_{\min} \equiv \sigma(m_{\min})$. We require that $df_{\text{new}}/dz \leq df_{\text{coll}}/dz$; the approximations in equation (2) violate this requirement at sufficiently high redshifts. The solid line associates m_{\min} with a virial temperature $T_{\text{vir}} = 10^4$ K. The dotted line assumes a value of m_{\min} that is an order of magnitude larger than this value, and the dashed line assumes it is an order of magnitude smaller. The figure reveals two important points. First, df_{new}/dz evolves slowly with redshift. It does not approach zero until $z \sim 6$, by which point reionization is complete. This is because m_{\min} is either larger than or close to the nonlinear mass scale at these early redshifts, so pristine galaxies are still forming. In fact, the magnitude of df_{new}/dz actually increases with cosmic time; its relative importance decreases only because the number of halos *larger* than the threshold increases even more rapidly (as they correspond to a higher value of ν), and each of these objects continues to accrete mass. Second, the fraction of mass entering new objects *increases* with increasing m_{\min} because such objects become rarer and it takes the nonlinear mass scale longer to reach a larger threshold. On the other hand, df_{new}/dz decreases somewhat more rapidly in this case.

Thus, without wind enrichment, we find that the transition between Pop III and Pop II star formation must be smooth and extend over a long redshift interval. It is difficult to imagine how sharp features in the reionization history could emerge from this kind of a transition.

2.2. The Extended Press-Schechter Estimate

As described above, equation (2) does not provide a rigorous estimate of df_{new}/dz . It is therefore useful to exam-

ine an alternate model and see if the same qualitative conclusions hold. Here we consider an estimate using the EPS formalism. Although the merger rates in this model are not entirely self-consistent, they form the basis for useful estimates in a variety of contexts, such as semi-analytic galaxy formation (e.g., Kauffmann & White 1993; Cole et al. 1994; Somerville & Kolatt 1999) and modeling the quasar luminosity function (e.g., Wyithe & Loeb 2002).

For a halo of mass m at redshift z_l , the EPS formalism provides the fraction of matter that was in objects with masses smaller than m_{\min} at some earlier time z_h (Lacey & Cole 1993) and hence the fraction of a halo's mass that was accreted recently:

$$F(< m_{\min}, z_h | m, z_l) = \text{erf} \left[\frac{\delta_c(z_h) - \delta_c(z_l)}{\sqrt{2(\sigma_{\min}^2 - \sigma_m^2)}} \right]. \quad (4)$$

The relevant timescale is the dynamical time within a galaxy (which gives approximately the time over which star formation occurs), $t_{\text{dyn}} \sim (G\rho)^{-1/2} \sim (\Delta_v \rho_c G)^{-1/2} \sim \sqrt{4/27\pi} H^{-1}(z)$, where $\rho_c = 3H^2/8\pi G$ is the critical density, $H(z)$ is the Hubble parameter at redshift z , and Δ_v is the virial overdensity (Barkana & Loeb 2001). The corresponding redshift interval is $z_h - z_l \approx (dz/dt)t_{\text{dyn}} = (1+z)H(z)t_{\text{dyn}} \sim (1+z)/5$. If we then assume that accretion onto halos with $m < 2m_{\min}$ can be included in the newly-formed halo component, we can estimate the fraction of collapsing gas that accretes directly onto existing halos via

$$f_{\text{old}} = \frac{\int_{2m_{\min}}^{\infty} dm m n(m) F(< m_{\min}, z_h | m, z_l)}{\int_{m_{\min}}^{\infty} dm m n(m) F(< m_{\min}, z_h | m, z_l)}, \quad (5)$$

so that $df_{\text{new}}/dz \approx (1 - f_{\text{old}})df_{\text{coll}}/dz$. The denominator is necessary to normalize the total mass accretion rate to its actual value; a direct calculation with the EPS merger rates of the total collapse rate does *not* reproduce the true df_{coll}/dz . One advantage of this formulation is that it includes the duration over which a new halo must remain isolated (unlike in equation [2]). In other words, a halo that merges into a massive object immediately after passing above m_{\min} will most likely form Pop II, rather than Pop III, stars. Unfortunately the relevant time interval is not defined precisely. In Figure 1 we have used the dynamical time to fix z_h . Varying the time offset has only a small effect on the results: increasing or decreasing t_{dyn} by a factor of two changes df_{new}/dz by $\lesssim 10\%$ and leaves the shape unaffected. Another approach is to use the explicit expression for $Q(m_1, m_2, z)$ in the EPS formalism to compute df_{new}/dz directly (but without the time offset). This procedure (with symmetrized EPS merger rates) yields results similar to equation (5) but must also be renormalized.

The resulting formation rate of new halos is shown in the bottom panel of Figure 1 for the same three mass thresholds as in the top panel. Interestingly, in this case df_{new}/dz evolves even more slowly than our standard calculation predicts: it falls below unity earlier and remains substantial much later. We thus conclude that df_{new}/dz , while unknown in detail, has the important property that it evolves slowly and smoothly with redshift, vanishing only at $z \lesssim 6$ for the mass thresholds of interest. We will conservatively continue to use equation (2); although inaccurate, this method appears to exaggerate the speed of the Pop III/Pop II transition and provide better prospects for double reionization (which, as shown later, is unlikely even under this favorable approximation).

3. WIND ENRICHMENT

In order for star formation to introduce a sharp feature into the reionization history, we must add more physics. Galactic winds are the most likely agent for spreading metals through the IGM (e.g., Aguirre et al. 2001; Madau et al. 2001; Scannapieco et al. 2002; Furlanetto & Loeb 2003) and for changing the characteristics of the Pop III/Pop II transition that was considered in the limited context of structure formation in §2. In this section we will quantify their significance.

3.1. Wind Model

Galactic winds are an extremely complex phenomenon that we do not yet fully understand. In order to keep our methods as straightforward as possible, we will examine a simple model for the wind expansion that captures the expected scaling laws and calibrate it against more advanced treatments.

We first consider the underlying energy budget of the winds. The available energy from supernovae is $W_{\text{SN}} = f_* f_w E_{\text{SN}} / \omega_{\text{SN}} m_b$, where f_* is the star formation efficiency (which may depend on halo mass), $E_{\text{SN}} = E_{51} \times 10^{51}$ erg is the energy per supernova, $\omega_{\text{SN}} = \omega_{100} \times 100 \text{ M}_\odot$ is the mass in stars per supernova event, and f_w is the fraction of the total supernova energy that enters the wind. The simplest possible model assumes an energy-conserving point explosion in a constant density medium. This well-known Sedov (1959) solution predicts that $R \propto (W_{\text{SN}} t^2 / \rho)^{1/5}$, where R is the radius, ρ is the density, and t is the elapsed time. Such a model neglects a number of important effects. One is the gravitational potential of the host halo. At large masses, gravity tends to flatten the mass dependence (Furlanetto & Loeb 2003). Another is radiative cooling, principally caused by inverse-Compton cooling off the CMB at the high redshifts of interest here. We can approximately include this effect by setting

$$f_w = \frac{t_{\text{comp}}}{t_H} \approx 0.6 \left(\frac{1+z}{10} \right)^{5/2}, \quad (6)$$

where t_{comp} is the Compton cooling time and $t_H \approx H^{-1}(z)$. (We set $f_w = 1$ if $t_{\text{comp}} > t_H$.) A third difficulty is in the definition of the elapsed time, because even halos of a fixed mass have a range of star formation histories (which we will normally associate with halo mergers, though our conclusions do not depend on this assumption so long as the stellar mass and halo mass are correlated through f_*). Crudely, we would expect more massive halos to be older, which steepens the mass dependence. On the other hand, the Sedov scaling also neglects the evolving background density (and the halo density profile). Older halos spend more time expanding into dense environments, which flattens the mass dependence. Finally, the scaling ignores the fact that the wind travels through an expanding medium, so that it need not accelerate swept up material from rest.

Fortunately, Furlanetto & Loeb (2003) showed that including all of these effects does not strongly affect the mass scaling. They found that $R \propto M^{1/5}$ describes the wind sizes at a fixed redshift reasonably well as long as the total wind energy is much greater than the binding energy of the host halo (so that gravity may be safely neglected). Massive halos for which gravity cannot be ignored are sufficiently rare that they do not contribute substantially to the enriched volume. For simplicity, we will therefore use the Sedov model for the distance that winds traverse. We will assume that each wind has propagated for half of the age of the universe, or $t \approx 1/3H(z)$.

Then we can write ξ , the ratio of total mass enriched by the wind to the mass of each galaxy, as

$$\xi(m) = 27 K_w \left(f_* f_w \frac{E_{51}}{\omega_{100}} \right)^{3/5} \left(\frac{m}{10^{10} M_\odot} \right)^{-2/5} \left(\frac{10}{1+z} \right)^{3/5}, \quad (7)$$

where f_w is to be evaluated through equation (6) and K_w is a normalization constant that accounts for the many factors we have neglected. Comparing to the results of Furlanetto & Loeb (2003), this solution yields radii 2–3 times too large, depending on the mass and redshift, suggesting that typical wind models have $K_w \sim \frac{1}{27} - \frac{1}{8}$. Note that in our calculations we actually take $1 + \xi(m)$ to include self-enrichment of the galaxy.

If the star formation efficiency is fixed, ξ increases with decreasing galaxy mass. However, there is some evidence that $f_* \propto \sigma^2 \propto m^{2/3}(1+z)$ in local galaxies with velocity dispersions $\sigma < \sigma_c \equiv 124 \text{ km s}^{-1}$ (Dekel & Woo 2003; Kauffmann et al. 2003); above this threshold the star formation efficiency remains constant. Interestingly, with this scaling ξ becomes independent of mass (at least below M_*). It is possible to construct reasonable reionization histories with both $f_* = \text{constant}$ and $f_* \propto \sigma^2$ (Wyithe & Loeb 2003a). We will consider both cases here; in the latter we take the redshift-dependent threshold to match equation (13) of Wyithe & Loeb (2003a), which we have called σ_c . When describing this scenario, we will quote $f_{*c} \equiv f_*(\sigma_c)$. For simplicity, we will assume $f_* \propto m^{2/3}$ even above the threshold; because such massive halos are so rare at high redshifts, this has a negligible effect on our results. In this scenario it may also appear that we must specify whether the Pop III star formation efficiency also varies with mass. However, because such stars form only in halos with $m \sim m_{\min}$, f_*^{III} is only relevant in halos of a particular mass. Thus we will quote f_*^{III} as a multiple of the Pop II star formation efficiency *in halos of the same mass*. For $f_* \propto m^{2/3}$, note that $f_*(m_{\min}) \approx 0.01 f_{*c}$.

In evaluating equation (7), we include both of the separate stellar populations, each of which can have different wind parameters and star formation efficiencies. To do the calculation rigorously, we would need to compute the fraction of stars produced in each mode in each halo, which is a function of each halo's merger history. For simplicity, we will instead assume that the fraction of Pop III stars is independent of halo mass and is given by $f_{\text{new}}/f_{\text{coll}}$, where f_{new} is the total mass fraction in Pop III stars integrated over time. This is rigorously true for $f_* \propto m^{2/3}$ (because ξ is then independent of mass), but it will underestimate the effects of Pop III stars if $f_* = \text{constant}$ because smaller mass halos have more Pop III stars and hence a larger ξ . Unfortunately a better treatment must await self-consistent merger rates or suitable numerical simulations.

Furlanetto & Loeb (2001) noted that we can set a maximal upper limit to the wind size by balancing the energy input with the energy required to accelerate the enclosed baryons to the Hubble velocity at the outer edge of the wind. This procedure yields $\xi_{\max} \approx 2.2\xi$ with exactly the same scalings as in equation (7). Thus the above estimate is reasonable; it is significantly smaller than the maximal limit because the winds have not completed their expansion. This also implies that we have not erred grossly in neglecting the Hubble flow based on the simple Sedov solution.

Finally, we have only included winds powered by supernovae. Quasars could also generate powerful winds fill-

ing a fair fraction of the IGM (see Furlanetto & Loeb 2001 and references therein); their relative importance will depend on the efficiency with which quasars and starbursts generate winds in the small halos common at high redshifts. Wyithe & Loeb (2003c) find a good fit to the quasar luminosity function over the range $z = 2\text{--}6$ by assuming that $M_{\text{bh}} \approx 10^5 M_\odot (\sigma/54 \text{ km s}^{-1})^5$. We can estimate how quasar winds affect the enrichment by assuming this relation extends to the higher redshifts and lower masses of interest. We will also assume that a quasar radiates a fraction ϵ_Q of its rest mass and that a fraction q_w powers the wind. For our constant star formation efficiency case, quasars make only a small difference to the results if $\epsilon_Q \sim q_w \sim 0.1$ because black holes can be ignored in the small halos responsible for most of the enrichment. However, if $f_* \propto m^{2/3}$, the supernova energy and quasar energy scale identically with halo mass. In this case we find the ratio of the total input energies to be

$$\frac{W_{SN}}{W_Q} \approx 0.1 \left(\frac{f_{*c}}{0.1} \frac{0.1}{q_w} \frac{0.1}{\epsilon_Q} \frac{E_{51}}{\omega_{100}} \right) \left(\frac{10}{1+z} \right)^{5/2}. \quad (8)$$

Clearly quasars can dominate the wind for reasonable parameters. However, because W_{SN}/W_Q is independent of halo mass, we can simply absorb the quasar energy into our normalization constant K_w . We will therefore consider a range of choices for this parameter well above the predictions of starburst wind models.

3.2. The Enrichment Probability

We now wish to compute the probability that a collapsing halo (with $m \approx m_{\min}$) forms in a region already enriched by galactic winds. As a first step, given the enrichment efficiency $\xi(m)$, we can estimate the fraction of space that winds have filled with metals:

$$Q'_e(z) = \int_{m_{\min}}^{\infty} dm \left(\frac{m}{\bar{\rho}} \right) \xi(m) n(m). \quad (9)$$

This equation would be accurate if the galactic winds did not overlap or if their volumes were additive (as is the case with H II regions, which occupy a net volume dictated by the total number of ionizing photons). However, because winds expand at much less than the speed of light, the latter is not a good approximation. If the host galaxies were randomly distributed, then the true filling factor of metals including overlap would be $p'_e = 1 - \exp(-Q'_e)$. We will use this expression; we discuss a more detailed model for overlap below.

Moreover, we actually wish to compute the probability that a new halo forms in an enriched region rather than the simple volume fraction of enriched material. Collapsing halos are biased and therefore lie near existing halos (and their winds). We will now try to estimate the importance of this effect. We first define m_w to be the average mass enclosed within the region occupied by a single galactic wind. We then smooth the density field on this scale and let $\sigma_w^2(z)$ be its variance at redshift z (without linear extrapolation to $z = 0$). We then ask the probability that a newly-formed halo falls within one of the enriched regions. In the large scale limit, the number density of halos as a function of local density is given by the linear bias formula, $n(m, \delta) = (1 + b\delta)n(m)$, where b is the bias parameter defined by Mo & White (1996). Here δ is the true density at the redshift of interest (again without linear extrapolation to $z = 0$).

We can then compute the probability that a newly-formed

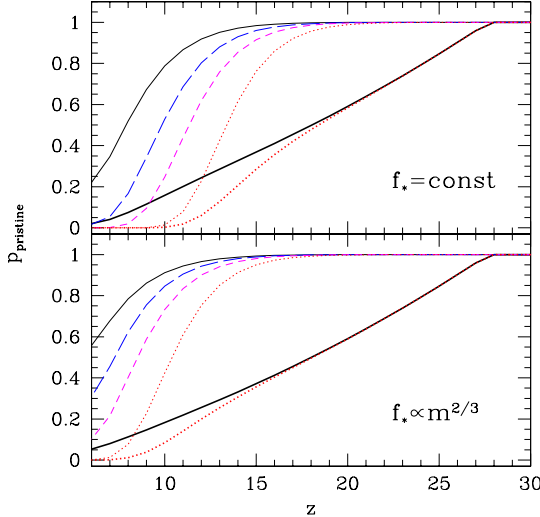


FIG. 2.— Probability that a new halo forms out of pristine gas (thin lines) and net fraction of collapsing gas that is able to form Pop III stars (thick curves). *Top*: $f_* = \text{constant}$ with $f_*^{\text{II}} = f_*^{\text{III}} = 0.1$. *Bottom*: $f_* \propto m^{2/3}$ with $f_{*c}^{\text{II}} = 0.1$ and $f_*^{\text{II}} = f_*^{\text{III}}$. The solid, long-dashed, short-dashed, and dotted curves assume $K_w^{1/3} = 1/3, 1/2, 2/3$, and 1, respectively. Otherwise, all lines assume our fiducial parameters (see text).

halo lies in an enriched region via

$$\begin{aligned} Q_e &= \int dm \xi(m) \int d\delta n(m, \delta) p(\delta) (1 + \delta b_{\text{new}}), \\ &= Q'_e (1 + b_{\text{new}} \bar{b}_w \sigma_w^2), \end{aligned} \quad (10)$$

where $p(\delta)$ is the density probability distribution, \bar{b}_w is the mean bias of a wind, and b_{new} is the bias of a newly-formed halo. In the first line, the last factor is the excess probability that a newly-formed halo is in a region of density δ ; without this part we would have $Q_e = Q'_e$. In the final line, we have assumed that $p(\delta)$ is Gaussian on the relevant scales. The mean bias of the enriched regions is easy to compute:

$$\bar{b}_w \equiv \frac{\int dm m \xi(m) b(m) n(m)}{\int dm m n(m)}, \quad (11)$$

where the extra factor of m enters because we compute the bias of the enriched *volumes* rather than the bias of halos. The bias of newly-formed galaxies is $b_{\text{new}} \approx b(m_{\text{min}})$ because all such objects have mass close to the low-mass threshold for star formation. We approximately include overlap of the winds by setting the enrichment probability $p_e = 1 - \exp(-Q_e)$.

Figures 2 and 3 show the resulting fraction of new halos that form in pristine environments in two sets of models. Figure 2 shows our fiducial model, which assumes $f_*^{\text{II}} = 0.1$ (or $f_{*c}^{\text{II}} = 0.1$), $E_{51}^{\text{II}} = 1$, $\omega_{100}^{\text{II}} = 1$, $f_*^{\text{III}} = f_*^{\text{II}}$, $E_{51}^{\text{III}} = 10$, and $\omega_{100}^{\text{III}} = 1$. Here the Pop II parameters are based on a Scalo (1998) IMF with stellar masses in the range $0.1\text{--}100 M_\odot$. The Pop III parameters assume that most of the stellar mass undergoes pair-instability supernovae, maximizing enrichment from the first generation (Heger & Woosley 2002). We also determine f_w based on equation (6), neglecting other energy loss channels. Simulations and observations of nearby winds actually suggest that $\gtrsim 50\%$ of the energy is lost by the wind (Strickland et al. 2000; Mori et al. 2002). We have

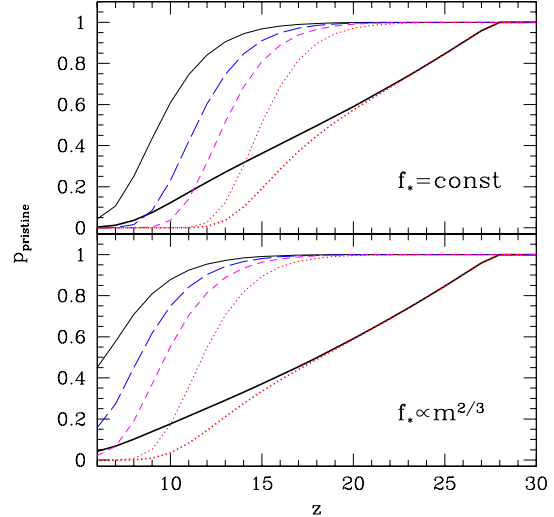


FIG. 3.— Same as Figure 2. *Top*: $f_* = \text{constant}$ with $f_*^{\text{II}} = 0.05$ and $f_*^{\text{III}} = 0.1$. *Bottom*: $f_* \propto m^{2/3}$ with $f_{*c}^{\text{II}} = 0.05$ and $f_*^{\text{III}} = 10f_*^{\text{II}}$. All other parameters are the same as our fiducial model (see text).

made the optimistic choice to maximize the enrichment and hence the prospects for double reionization. Figure 3 increases the Pop III star formation efficiency. In each case, the thin lines show $p_{\text{pristine}} \equiv 1 - p_e$, while the thick lines show the total fraction of collapsing gas able to form Pop III stars, $p_{\text{pristine}}(df_{\text{new}}/dz)/(df_{\text{coll}}/dz)$. We find that with strong winds ($K_w = 1$) enrichment completes at $z \sim 12$ for $f_* = \text{constant}$ and at $z \sim 8$ for $f_* \propto m^{2/3}$. With more realistic choices for K_w , enrichment occurs significantly later and may not be complete by $z \sim 6$, although quasar winds could move the enrichment epoch to earlier times (especially if f_* is mass-dependent). For $f_* \propto m^{2/3}$, the total fraction of collapsing material able to form Pop III stars is nearly independent of the enrichment history and is almost entirely controlled by df_{new}/dz . Finally, we note that the bias amplification of equation (10) turns out to be relatively modest in the regime of interest. By the time Q_e has become large, the bias typically increases p_e by only $\sim 25\%$.

We end this section by noting a number of caveats about our simplified treatment. The most serious shortcoming of equation (10) is that it does not rigorously account for wind overlap. In particular, we have made no attempt to follow the dynamics of colliding winds. However, since the wind volume scales with the deposited energy more slowly than linearly, combining their energies through overlap will only reduce the total enriched volume relative to a case without overlap. Thus the net effect of overlap is to *slow* the transition from Pop III to Pop II and therefore strengthen our conclusions in §4. Second, we have assumed that galaxy formation in the wind-enriched regions can be well-described by dark matter dynamics. This may not be a good assumption if the winds disturb a large fraction of the IGM by, for example, sweeping it into a shell, stripping nearby halos as they collapse, or triggering star formation behind the termination shock (Scannapieco et al. 2001; Cen 2003c). If the feedback is positive, double reionization would become even more difficult, but if the winds suppress galaxy formation the prospects for double reionization would be enhanced. (That case would be qualitatively similar to photoheating, except

that the feedback would operate much more slowly.) Third, we have assumed that winds have a single scale, while they actually have a range of sizes (especially if overlap is included). Fortunately, this choice is not crucially important because σ varies gently over the relevant range of scales.

Finally, there is a set of issues related to our simplified global treatment of enrichment. Equation (10) includes the halo bias only approximately. One reason is that it assumes a Gaussian density distribution and linear bias; in reality, winds at high redshifts do not extend far beyond the virial radius of their host galaxies and so these assumptions probably break down. We have also treated the distribution of galaxies as random for the purpose of calculating the overlap probability. Scannapieco et al. (2003) constructed a more detailed model that included aspects of all these issues. They used the two-point halo mass function (Scannapieco & Barkana 2002) to compute the probability that a halo lies within the winds of its neighbors. They found that the enrichment history is even more extended than in our models (similar to the EPS curves in Fig. 1). The reason is essentially that the Scannapieco & Barkana (2002) formalism is built from the EPS approach (and so it suffers from the same limitations). Our results are qualitatively consistent with theirs, so the non-linear corrections included by this formalism do not seem to affect our conclusions. However, neither approach includes all the relevant physics, such as overlapping winds and the fully nonlinear density field. All of these issues are best addressed with numerical simulations, which we forego in order to keep our models as simple as possible.

4. METAL ENRICHMENT AND THE REIONIZATION HISTORY

We next examine how enrichment, and the accompanying transition from Pop III to Pop II star formation, affects reionization. The rates at which Pop III and Pop II stars form are

$$\frac{df_{\text{III}}}{dz} = p_{\text{pristine}}(z) \frac{df_{\text{new}}}{dz} \quad (12)$$

and

$$\frac{df_{\text{II}}}{dz} = \frac{df_{\text{coll}}}{dz} - \frac{df_{\text{III}}}{dz}. \quad (13)$$

To translate these into production rates of ionizing photons, we define ζ_i as the number of ionizing photons produced per collapsed baryon for Pop i (where $i = \text{II}$ or III), e.g. $\zeta_i = A_{\text{He}} f_{\star}^i f_{\text{esc}}^i N_{\gamma b}^i$, where f_{esc} is the fraction of ionizing photons able to escape the host halo, $N_{\gamma b}$ is the number of ionizing photons produced per baryon incorporated into stars, and A_{He} corrects for helium.

If the values of ζ_i are independent of mass, the number of ionizing photons emitted per baryon per unit redshift is simply

$$\epsilon(z) = \zeta_{\text{II}} \frac{df_{\text{II}}}{dz} + \zeta_{\text{III}} \frac{df_{\text{III}}}{dz}. \quad (14)$$

However, if $\zeta = \zeta(m)$ (as, for example, in the case where $f_{\star} \propto m^{2/3}$) the calculation is more subtle because the stellar mass increases during mergers even though the collapse fraction has not changed. Moreover, the rate at which collapsing gas produces ionizing photons depends on the distribution of accretion rates among existing halos. Obviously the calculation requires self-consistent merger rates, which are not available in analytic forms (see the discussion in §2.1). We will therefore adopt a simple approximate approach. We first define the mass-averaged ionizing efficiency

$$\bar{\zeta}_{\text{II}} = \frac{\int dm \zeta_{\text{II}}(m) mn(m)}{\int dm mn(m)}, \quad (15)$$

which is a function of redshift as the mass function changes (if $f_{\star} \propto m^{2/3}$, the evolution is substantial over the range $30 > z > 6$). We then assume that material accretes onto existing halos in proportion to their mass, i.e. $\bar{\zeta}_{\text{II}}$ describes not only the cumulative emissivity of gas already in halos but also the average emissivity of newly accreting gas. With this simplification, the emissivity is

$$\epsilon(z) = f_{\text{coll}} \frac{d\bar{\zeta}_{\text{II}}}{dz} + \bar{\zeta}_{\text{II}} \left(\frac{df_{\text{coll}}}{dz} - \frac{df_{\text{new}}}{dz} \right) + \frac{df_{\text{new}}}{dz} [\zeta_{\text{II}}(m_{\text{min}})(1 - p_{\text{pristine}}) + \zeta_{\text{III}} p_{\text{pristine}}]. \quad (16)$$

Here the first term describes stars created during mergers, the second describes mass accreted onto existing halos, and the third describes newly-formed halos. To check the accuracy of our approximation for the distribution of accretion with halo mass, we note that it will cause an error in the total, time-integrated emissivity (and hence in the stellar mass). We have ensured that our prescription yields the correct mass to within $\sim 15\%$ for the models we consider, so it will suffice for our purposes.

Given the emissivity, we can compute the evolution of the global ionized fraction \bar{x}_i via (Shapiro & Giroux 1987; Barkana & Loeb 2001)

$$\frac{d\bar{x}_i}{dz} = \epsilon(z) - \bar{x}_i \alpha_B n_e C (1+z)^3 \left| \frac{dt}{dz} \right|, \quad (17)$$

where α_B is the case-B recombination coefficient, n_e is the comoving electron density in a fully ionized medium, and C is the density clumping factor within ionized regions. The first term is the rate at which stars produce ionizing photons, while the second is the rate at which protons and electrons recombine. We treat C as a constant; a better model would include the evolving density distribution of ionized gas in the IGM. Miralda-Escudé et al. (2000) have developed such a model calibrated to numerical simulations. They argue that low-density regions, where the recombination rate is small, will be ionized first. As the ionized volume increases, the ionizing background can keep progressively denser regions ionized. Although C increases throughout reionization, its value does not change significantly until \bar{x}_i is relatively large, because nearly all of the volume is near the mean density at the high redshifts of interest. Since we are primarily interested in the middle phases of reionization, the assumption of a constant C is reasonable unless there is considerably more small-scale structure than the simulations of Miralda-Escudé et al. (2000) found (e.g., Haiman et al. 2001).

It is important to keep in mind that our scheme breaks down when \bar{x}_i approaches unity. In the model of Miralda-Escudé et al. (2000), C increases rapidly as $\bar{x}_i \rightarrow 1$, ensuring that the ionized fraction never exceeds unity. To mimic this behaviour we explicitly force $\bar{x}_i \leq 1$ when necessary. A more serious problem is that by underestimating the clumping factor in dense regions, we underestimate the likelihood that recombinations exceed ionizations in some fraction of the IGM. Although most of the volume may remain ionized after the Pop III/Pop II transition, some sufficiently dense regions will recombine if $\zeta_{\text{II}} < \zeta_{\text{III}}$ (see below). Here we focus on the possibility that a major fraction of the IGM recombines, a phenomenon which is much more easily observable. For this problem our approximation is adequate.

Figures 4 and 5 illustrate reionization in two sets of models. The top panels show the evolution of $\epsilon(z)$ and the bottom panels show $\bar{x}_i(z)$. Figure 4 uses the same parameters as

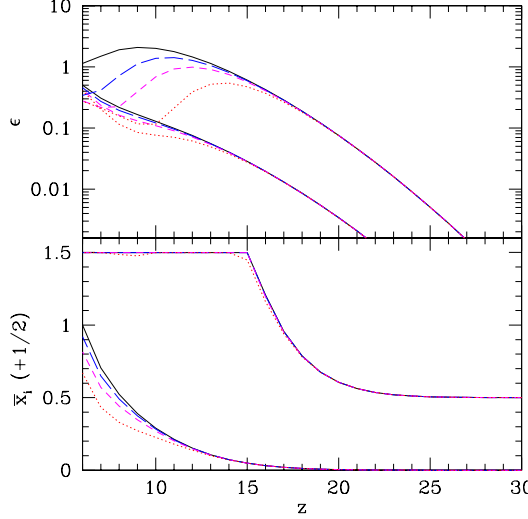


FIG. 4.— Reionization histories. *Top*: Normalized emissivity. *Bottom*: Ionized fraction. In each panel the upper set of curves assumes $f_* = \text{constant}$ and the bottom set assumes $f_* \propto m^{2/3}$ and $f_{\text{esc}}^{\text{III}} = 1$. In the former case we plot $(\bar{x}_i + 0.5)$ for clarity of presentation. The corresponding enrichment histories are shown in Figure 2. The solid, long-dashed, short-dashed, and dotted curves assume $K_w^{1/3} = 1/3, 1/2, 2/3$, and 1, respectively.

Figure 2 and additionally assumes: $f_{\text{esc}}^{\text{II}} = 0.05$, $N_{\gamma b}^{\text{II}} = 4000$, $N_{\gamma b}^{\text{III}} = 30,000$, and $C = 1$. The upper set of curves assume $f_* = \text{constant}$ and $f_{\text{esc}}^{\text{III}} = 0.05$, so that the only difference between the modes is in the value of $N_{\gamma b}$, which is much larger for massive Pop III stars (Bromm et al. 2001b). The lower set of curves assumes $f_* \propto m^{2/3}$ and $f_{\text{esc}}^{\text{III}} = 1$. In this case we have further increased $\zeta_{\text{III}}/\zeta_{\text{II}}$ because f_* is small near m_{min} , but there is some physical motivation for this choice (Whalen et al. 2004). Within each set, we vary the wind efficiency from $K_w^{1/3} = 1$ to $K_w^{1/3} = 1/3$.

Figure 2 indicates that in the $f_* = \text{constant}$ case, reionization occurs at $z \sim 15$ while enrichment occurs at $z \lesssim 12$. Thus, until reionization is complete enrichment is not important and the emissivity increases monotonically. Only after reionization is complete (when $d\chi_{\text{III}}/dz \approx 0$) does the emissivity decrease until $\epsilon(z) \approx \zeta_{\text{II}} d\chi_{\text{coll}}/dz$. After that point, the emissivity begins to rise again because the collapse rate increases monotonically with time. Although ϵ falls by a factor of ~ 5 , the bottom panel shows that the intergalactic hydrogen remains fully (or nearly fully) ionized even as the emissivity drops. This is because *maintaining* full ionization requires only that the production rate of ionizing photons exceeds the rate at which hydrogen atoms recombine (i.e., the right-hand side of equation (17) must be positive). Thus \bar{x}_i will only decrease with time if

$$\epsilon(z) \lesssim 0.1 C \bar{x}_i \left(\frac{1+z}{10} \right)^{1/2}. \quad (18)$$

The marked decrease in the emissivity in Figure 4, although large in relative terms, is still insufficient for recombinations to dominate. Of course, this is only true in regions where C is near unity; sufficiently dense regions may recombine. For example, Miralda-Escudé et al. (2000) argue that the lowest density gas is always ionized first. In such a picture, the density threshold for neutral gas would fall following the Pop III/Pop II transition, but because the vast majority of the IGM

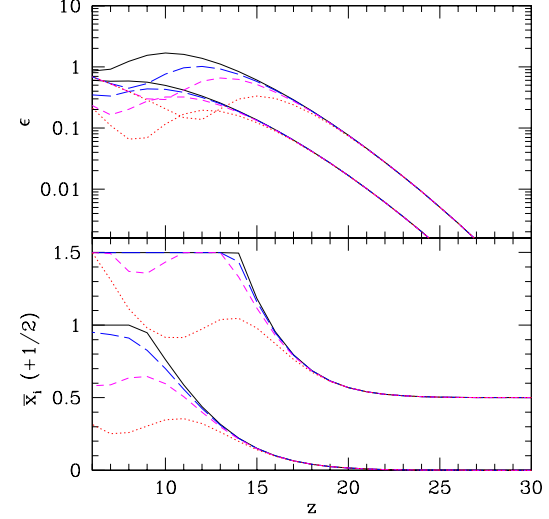


FIG. 5.— Same as Figure 4 except for different model parameters. The curves with $f_* \propto m^{2/3}$ have $f_{\text{esc}}^{\text{II}} = 0.05$, $f_{\text{esc}}^{\text{III}} = 10f_*^{\text{II}}$, $f_{\text{esc}}^{\text{III}} = 1$, and $C = 3$. The curves with $f_* = \text{constant}$ have $f_*^{\text{II}} = 0.05$, $f_*^{\text{III}} = 0.1$, $f_{\text{esc}}^{\text{III}} = 0.2$, and $C = 3$. The corresponding enrichment histories are shown in Figure 3.

is near the mean density, only a small fraction would recombine. On the other hand, this model neglects the bias of dense clumps, which presumably lie relatively close to the ionizing sources and so probably remain ionized longer. We will briefly discuss the resulting distribution of ionized gas in §6 below.

The case with $f_* \propto m^{2/3}$ shows a different behavior. The most obvious difference, of course, is that reionization occurs much later because nearly all galaxies have $f_* \ll 0.1$. More importantly for our purposes, the emissivity remains monotonic and, in fact, the shape only changes significantly if winds are maximal with $K_w = 1$. Again, this is partly because the star formation efficiency is small if $m \sim m_{\text{min}}$, and even the increased ionizing efficiency of Pop III stars (150 times larger than Pop II stars in the same halos) is not sufficient for them to dominate the ionizing photon budget at $z \lesssim 10$. This is principally because the fraction of gas accreting directly onto existing halos is near unity by this time (see Figure 1). If the real accretion rate is closer to the EPS model, the curves differ by a somewhat larger amount, although the emissivity remains monotonic. Interestingly, quasars can strongly affect the ionization and enrichment histories in this case. If they do exist in small halos, we expect K_w to be in the upper range of the plotted curves. However, they would also increase ζ_{II} by a substantial amount (Wyithe & Loeb 2003a): the net effect would be to shift the curves to higher redshift, so enrichment would still be unlikely to cause double reionization.

The above results have important implications for the star formation efficiency required for early reionization that stretch beyond the restricted goal of this paper. If $f_* \propto m^{2/3}$, $f_*^{\text{III}} = f_*^{\text{II}}$, and Pop III stars only form in halos with $m \sim m_{\text{min}}$, then early reionization at $z \gg 6$ requires a large $f_{\text{esc}}^{\text{III}}$. For example, the histories with $f_* \propto m^{2/3}$ in Figure 4 all have an optical depth to electron scattering $\tau_{\text{es}} \lesssim 0.07$; even with $f_{\text{esc}}^{\text{III}} = f_{\text{esc}}^{\text{II}} = 1$, we still get $\tau_{\text{es}} \lesssim 0.1$. Previous studies, such as Wyithe & Loeb (2003a), had found otherwise because they allowed larger halos to form Pop III stars even though such galaxies would have been enriched by their progenitors. Thus,

if observations continue to favor early reionization, it appears the star formation efficiency must scale differently with mass than in nearby galaxies, at least for one of the two star formation modes, or that quasars dominate the ionizations (a scenario disfavored by the soft X-ray background; Dijkstra et al. 2004b).

Figure 5 shows histories for another set of model parameters in which we have sharpened the contrast between Pop III and Pop II stars as well as increased the clumping factor to $C = 3$. For the curves with $f_* = \text{constant}$, we take $f_*^{\text{II}} = 0.05$, $f_*^{\text{III}} = 0.1$, and $f_{\text{esc}}^{\text{III}} = 0.2$. For $f_* \propto m^{2/3}$, we take $f_{*c}^{\text{II}} = 0.05$, $f_*^{\text{III}} = 10f_*^{\text{II}}$, and $f_{\text{esc}}^{\text{III}} = 1$. The purpose of these choices is to strengthen the drop in emissivity following enrichment and to speed up recombinations. Indeed, with these choices we see that both the emissivity and ionized fraction can decrease with time, but *only* if winds are more efficient than expected from detailed studies such as Furlanetto & Loeb (2003), which had $K_w^{1/3} \lesssim 1/2$. The emissivity drops by a somewhat larger relative factor than before and, because $C = 3$, also falls below the recombination threshold in equation (18). With the same parameters except $C = 1$, \bar{x}_i remains monotonic for all $K_w \leq 1$. Thus, provided that $C \approx 1$ throughout most of the IGM, even this optimistic case cannot lead to noticeable double reionization.

The principal lesson of this section is that double reionization is extremely difficult to achieve in realistic wind models. For either of our star formation laws, it requires $\zeta_{\text{III}} \gg \zeta_{\text{II}}$ (and in particular larger than the expected difference in $N_{\gamma b}$; Bromm et al. 2001b), a large clumping factor in order to reduce the recombination time in the IGM, and a wind efficiency considerably larger than predicted from semi-analytic models. Otherwise, either (i) the enrichment is not sufficiently extensive for a rapid Pop III/Pop II transition or (ii) the transition occurs only after Pop II stars are able to maintain ionization on their own throughout most of the IGM (wherever $C \sim 1$). The gentle decline in df_{new}/dz is not sufficient to induce double reionization.

5. RADIATIVE FEEDBACK

The second type of feedback mechanism is radiative, for which the most important example is photoionization heating. As described in §1, such heating raises the Jeans mass in ionized regions, but the precise degree to which photoionization suppresses structure formation remains somewhat uncertain. Our primary interest is in whether this feedback mechanism can cause double reionization; we will therefore take a phenomenological approach and leave the minimum galaxy mass in heated regions as a free parameter. Because the physics depends on the depth of the potential well, we will phrase the threshold in terms of a (redshift-independent) virial temperature T_h . We will also let $T_c = T_{\text{vir}}(m_{\text{min}})$; the h and c subscripts refer to hot and cold gas, respectively. We will take $T_h = 2.5 \times 10^5$ K as a fiducial value, corresponding to $V_c \approx 50$ km s $^{-1}$. As also mentioned in §1, a similar radiative feedback mechanism operates at lower virial temperatures through the photodissociation of H₂ molecules. We will consider this possibility in §5.1.

A number of authors have already included photoionization heating in models of reionization (e.g., Wyithe & Loeb 2003a; Cen 2003a; Somerville & Livio 2003; Onken & Miralda-Escudé 2004), although its role in allowing double reionization has not been examined

systematically. In this case the emissivity has two terms:

$$\epsilon(z) = x_h \frac{d\langle \zeta f_h \rangle}{dz} + (1 - x_h) \frac{d\langle \zeta f_c \rangle}{dz}, \quad (19)$$

where x_h is the filling factor of regions that have been heated by photoionization, $f_h \equiv f_{\text{coll}}(> T_h)$, and $f_c \equiv f_{\text{coll}}(> T_c)$. We take the derivative of the mass-averaged ionizing rate for each component, $\langle \zeta f_h \rangle$ and $\langle \zeta f_c \rangle$, rather than of the simple collapse fractions because the effective ionizing efficiency evolves if the star formation efficiency is a function of halo mass (see the discussion preceding equation [16]). We may then insert this emissivity into equation (17) and solve for $\bar{x}_i(z)$.

However, to do so we must specify $x_h(z)$. The simplest assumption, and one often used in the literature, is to set $\bar{x}_i = x_h$: the fraction of gas that has been heated is the same as the ionized fraction. Unfortunately, this is *not* a good assumption and will tend to stretch the duration of the transition (thus washing out any sharp double reionization features). Suppose $T_h \gg T_c$, so that the emissivity in hot regions is negligible. The first halos (with $T_{\text{vir}} = T_c$) collapse and ionize their surroundings; structure formation effectively stops in these ionized bubbles. However, small halos can continue to form in the neutral gas outside these bubbles. Thus ionizing photons will preferentially appear in *cold* regions while recombinations will only occur in *hot* regions. The filling factor of hot gas must therefore evolve faster than \bar{x}_i . We can approximate such a scenario by calculating x_h without including any recombinations:

$$\frac{dx_h}{dz} = \epsilon(z). \quad (20)$$

While we regard equation (20) as a more accurate description than setting $x_h = \bar{x}_i$, reality lies somewhere between these two extremes: some fraction of the ionizing photons are produced in pre-ionized regions and counteract recombinations before ionizing new material, while recombinations also occur in the newly-formed ionized bubbles. Furthermore, the medium cools adiabatically after the initial ionization, which begins to soften the increase in the time-averaged Jeans mass (or “filter mass”; Gnedin & Hui 1998). Cen (2003a) has included these effects more precisely through a “phase-space” description. We adopt equation (20) in determining $\bar{x}_i = x_h$ since it maximizes the prospects for double reionization. The regime in which equation (20) breaks down is where $T_h \sim T_c$, so that structure can continue to form in ionized regions without a significant pause. In this case double reionization is clearly impossible anyway.

Figure 6 shows the reionization history for a set of models with $\zeta = 100$ and $f_* = \text{constant}$ (note that we only consider a single stellar population here). The solid, long-dashed, short-dashed, and dotted curves have $T_h = 10^4, 10^5, 2.5 \times 10^5$, and 10^6 K, respectively, with $C = 1$. The dot-dashed curve has $T_h = 2.5 \times 10^5$ K and $C = 3$. In this case, the emissivity is the same as for the short-dashed curve. The solid curve shows the ionization history without photoheating; it rises steeply, completing reionization in a relatively short time period. An increase in T_h/T_c , introduces a stronger break into the emissivity. As long as $x_h \ll 1$, small halos dominate the ionizing photon budget and the evolution is nearly independent of T_h/T_c . Once x_h becomes large, $\epsilon \propto d\langle \zeta f_h \rangle/dz$ and T_h determines the amplitude as well as the duration of the break. Note that the redshift at which $x_h = 1$ corresponds to the minimum in ϵ . Equation (18) again expresses the criterion for double reionization: the emissivity must fall below the recombination rate. Thus, larger clumping factors or earlier reionization makes double reionization somewhat easier to achieve.

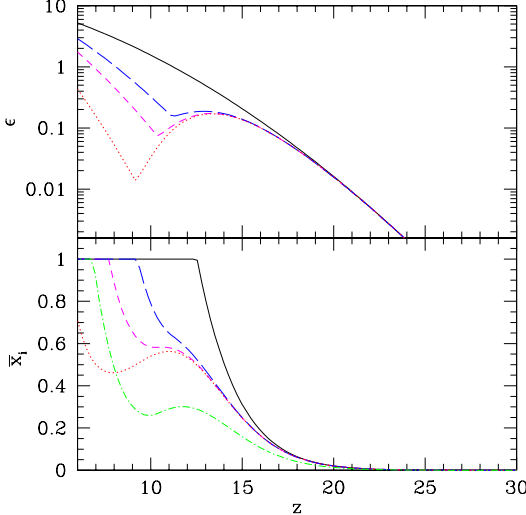


FIG. 6.— Same as Fig. 4, but for models in which photoionization heating raises the mass threshold for collapse. All curves assume $\zeta = 100$ and $f_* = \text{constant}$. The solid, long-dashed, short-dashed, and dotted curves have $T_h = 10^4, 10^5, 2.5 \times 10^5$, and 10^6 K, respectively, with $C = 1$. The dot-dashed curves have $T_h = 2.5 \times 10^5$ K and $C = 3$; in this case the emissivity is the same as the short-dashed curve.

Interestingly, the fiducial choice $T_h = 2.5 \times 10^5$ K is just on the threshold for achieving double reionization. If photoheating suppression is less important near the time of reionization (Dijkstra et al. 2004a), double reionization would require an abnormally high clumping factor for the IGM.

Another interesting result is that the character of double reionization differs between the metal enrichment and photoheating prescriptions. In the former case, winds travel much slower than ionizing photons, so the transition between star formation modes occurs *after* reionization has already been completed, unless a large clumping factor delays reionization. With photoheating, the transition occurs *before* reionization because $x_h > \bar{x}_i$. Thus the recombination phase precedes the point at which $\bar{x}_i = 1$, and the double ionization phase occurs early in the process. (Of course, complete heating does require every point to have been ionized at least once, but different points need not be ionized simultaneously.) These conclusions are robust to uncertainties in our model parameters and appear to be generic signatures of the different types of feedback.

Figure 7 shows reionization histories for models with $f_* \propto m^{2/3}$ and $\zeta_c = 500$ (evaluated at the fiducial σ_c). In this case the behavior is obviously quite different, with \bar{x}_i remaining monotonic in all cases. Even for the most extreme choice of T_h/T_c , $\epsilon(z)$ exhibits only a slight turnover. The difference arises because the star formation efficiency in low-mass halos is small to start with, making their contribution to the global emissivity low. The decline in emissivity is much less severe in this case, and double reionization requires extreme parameters. This also implies that if quasars are important in reionization and $M_{\text{bh}} \propto \sigma^5$, they will tend to wash out double reionization because massive halos contribute a large fraction of the ionizations.

Finally, we note that we are unable to find *any* set of parameter choices in which the ionized fraction decreases with cosmic time if we take $x_h = \bar{x}_i$. In this case the emissivity is regulated by the instantaneous ionized fraction, so there is

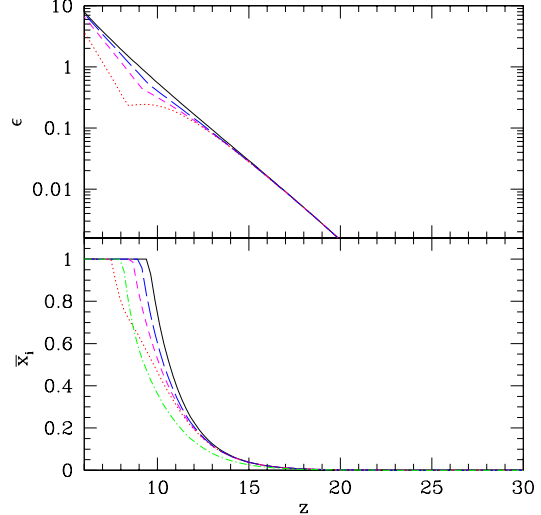


FIG. 7.— Same as Fig. 6, except $\zeta_c = 500$ and $f_* \propto m^{2/3}$.

no possibility of an “overshoot” in \bar{x}_i . This explains why our treatment of photoionization heating yields some possibility of double reionization while others in the literature do not.

5.1. Photodissociation of H_2

As described briefly in §1, gas in the first collapsed halos cools through rotational transitions of H_2 (Haiman et al. 1996; Tegmark et al. 1997), which operate for $T_{\text{vir}} \gtrsim 200$ K. However, such molecules are fragile and a weak soft UV background of $J_{21} \gtrsim 10^{-3}$ suffices to dissociate them, where $J_\nu \equiv J_{21} \times \text{erg cm}^{-2} \text{ s}^{-1} \text{ Hz}^{-1} \text{ sr}^{-1}$ (Haiman et al. 2000; Machacek et al. 2001). Crucially, any photon with energy above 11.26 eV can dissociate H_2 , so (unlike in the case of ionizing photons) any individual halo sees Lyman-Werner sources out to cosmological distances (Haiman et al. 1997). The UV background redward of the Lyman limit builds up quickly as stars form, suppressing cooling via H_2 and increasing the minimum halo mass for star formation from $T_c \sim 200$ K to the atomic cooling threshold of $T_h = 10^4$ K.

Because the effects of H_2 photodissociation can be phrased in the same way as photoheating, we can again find scenarios in which \bar{x}_i decreases with cosmic time, as long as the clumping factor is substantial, $T_h/T_c \gg 1$, or we consider sufficiently high redshifts. However, it is easy to show that this phase occurs early in the reionization process, because the photodissociation threshold *must* be reached well before reionization is completed (Haiman et al. 2000). We wish to estimate J_ν in the Lyman-Werner bands; neglecting the line opacity of the IGM, we have

$$J_\nu = \frac{c}{4\pi} \int_z^{z_{\text{max}}} dz' \frac{dt}{dz'} \epsilon_{\text{LW}}(\nu') \frac{1+z}{1+z'}, \quad (21)$$

where ϵ_ν is the emissivity per unit frequency, $\nu' = \nu(1+z')/(1+z)$, and the last factor accounts for the cosmological redshifting of the photon energy. The upper limit z_{max} enters because ionizing photons cannot propagate through the neutral IGM. The Lyman series introduces a “sawtooth modulation” of the background (Haiman et al. 1997), but this does not affect our estimate. To connect to the ionized fraction, we write $\epsilon_{\text{LW}}(\nu) = h\nu \times (1/\nu) \times \chi n_{\text{ion}}$, where n_{ion} is the rate

at which ionizing photons are produced per unit volume and χ is the number of Lyman-Werner photons per frequency decade divided by the number of ionizing photons per frequency decade.³ Ciardi & Madau (2003) have evaluated a closely related quantity and found $\chi \sim 10^{0.4}-10^{1.2}$ for typical stellar populations (the only difference is that they calculated the number of continuum photons just shortward of Ly α rather than shortward of 11.26 eV). Thus using our earlier definitions, we have

$$J_\nu \approx \frac{ch}{4\pi} \chi \bar{n}_b(z) f_\star N_{\gamma b} \Delta f_{\text{coll}}, \quad (22)$$

where $\bar{n}_b(z)$ is the mean baryon density and $\Delta f_{\text{coll}} = f_{\text{coll}}(z) - f_{\text{coll}}(z_{\text{max}})$. Neglecting recombinations, we can then write $\bar{x}_i = f_\star f_{\text{esc}} N_{\gamma b} f_{\text{coll}}$, so the ionized fraction \bar{x}_m when we reach the photodissociation threshold $J_{m,21}$ is

$$\bar{x}_m \approx 0.03 \left(\frac{f_{\text{esc}}}{\chi} \right) \left(\frac{J_{m,21}}{0.1} \right) \left(\frac{f_{\text{coll}}}{\Delta f_{\text{coll}}} \right) \left(\frac{1+z}{10} \right)^3. \quad (23)$$

Even with $f_{\text{esc}} = 1$, $\chi = 1$, and $f_{\text{coll}} \approx 3\Delta f_{\text{coll}}$, the ionized fraction is at most several percent when we reach the photodissociation threshold. This estimate agrees with the detailed models of Haiman et al. (2000) (their Figure 7). Thus although this mechanism can cause \bar{x}_i to turn over, it can only do so near the beginning of reionization and the absolute amplitude of the change will be small.

Finally, we note that in reality the chemistry of H₂ is sufficiently complicated that the detailed consequences of radiative feedback remain unclear. Initially it was thought that X-rays could catalyze its formation by increasing the free electron fraction (Haiman et al. 2000); however, Oh & Haiman (2003) showed that the heating that inevitably accompanies X-rays impedes collapse, ensuring a net suppression. Others have argued for more complicated positive feedback mechanisms near H II regions (Ricotti et al. 2002; Cen 2003a). We will ignore all of these possibilities simply because positive feedback obviously cannot cause double reionization. Finally, the “self-regulation” process will not necessarily completely halt the formation of low-mass halos. If small halos are responsible for the background, they will reach an equilibrium in which the UV background prevents the smallest halos from forming stars but allows more massive and better shielded halos to cool. Again, such a scenario tends to wash out double reionization.

6. THE TOPOLOGY OF H II REGIONS

One promising observable of the reionization process is the size distribution of H II regions and its evolution with time (FZH04; Wyithe & Loeb 2004c), which can be probed through 21 cm tomography (Furlanetto et al. 2004c) or through Ly α absorption (Furlanetto et al. 2004a; Wyithe & Loeb 2004b). By modulating the ionizing efficiency through local feedback mechanisms, the schemes we have described can in principle have substantial effects on the size distribution of ionized bubbles. Here we will briefly discuss those consequences. Furlanetto et al. (2004c) made some progress in this direction by considering simple scenarios with multiple generations of sources. We will improve on that treatment by examining the transition between star formation modes in more detail.

³ We will assume for simplicity that all of the ionizing photons are contained in the frequency decade closest to the Lyman limit, which is a good approximation for stellar spectra. Even if the ionizing sources have hard spectra similar to quasars, our conclusion would not change.

We take the model of FZH04 as a starting point. We assume as above that the number of ionizing photons produced in a region is proportional to the collapse fraction within the region. We denote the proportionality constant by ζ . Note that this differs from the definition in §4 in two ways: it is cumulative over the integrated star formation history and it includes a correction for past recombinations. A region can ionize itself if $\zeta f_{\text{coll}} > 1$. FZH04 showed how to transform this simple condition into a size distribution by including the implicit scale dependence of f_{coll} and ionizations from neighboring regions. We rewrite the ionization constraint as a condition on the density,

$$\delta_m \geq \delta_x(m, z) \equiv \delta_c(z) - \sqrt{2}K(\zeta)[\sigma_{\text{min}}^2 - \sigma^2(m)]^{1/2}, \quad (24)$$

where $K(\zeta) = \text{erf}^{-1}(1 - \zeta^{-1})$, $\delta_c(z)$ is the critical density for virialization, and $\sigma(m)$ is the mass variance smoothed on scale m . Equation (24) is then used as an absorbing barrier within the excursion set formalism (Bond et al. 1991; Lacey & Cole 1993) to construct the mass function of ionized bubbles. The crucial point is that the *shape* of the barrier determines the distribution of bubble sizes. The above barrier is nearly linear in σ^2 , which implies (Sheth 1998) a well-defined characteristic size for the H II regions. Thus, the shape of the barrier is fixed by the condition $f_{\text{coll}} = \text{constant}$, while the normalization is fixed by the ionizing efficiency.

We may now incorporate feedback by considering two sets of sources with different ionizing efficiencies and/or different galaxy mass thresholds. In the latter case (i.e., photoionization heating), the qualitative effects are easy to guess. A high-density region forms halos with $T_{\text{vir}} \approx T_c$ which ionize the neighborhood. Without feedback, the associated bubble would grow rapidly through two processes: (i) it would merge with other H II regions, and (ii) halos inside it would continue to grow rapidly, producing more ionizing photons. However, if $T_h \gg T_c$, structure formation is suppressed in this region, the “internal” ionizations diminish, and the bubble can grow only by merging with its neighbors. Thus we would expect H II regions to be *smaller* and more numerous, because those around high-density regions grow more slowly and force voids to be ionized by the relatively rare galaxies embedded inside. At the same time, the high-density dormant regions begin to recombine. Furlanetto et al. (2004c) argued that this process would not stop until the entire universe had been ionized, though not necessarily simultaneously (see §5), so eventually the pattern induced by recombinations (and exaggerated by the time delay between reionization in different regions) would dominate the signal. Unfortunately, because the photoheating depends directly on the ionized fraction, it cannot be incorporated into the FZH04 model.

However, the FZH04 model can accommodate a transition due to metal enrichment more easily, because the ionizing efficiency does not depend on the local ionized fraction in this case. We will assume that there exists a function $p_{\text{II}}(\delta)$ characterizing the probability that any source in a region of overdensity δ contains Pop II stars. Physically plausible models will have $p'_{\text{II}} > 0$, where a prime denotes the derivative with respect to density, because structure formation is more advanced in dense regions. Given the ionizing efficiency of each star formation mode, the condition for self-ionization is

$$f_{\text{coll}}(\delta) [(\zeta_{\text{II}} - \zeta_{\text{III}})p_{\text{II}}(\delta) + \zeta_{\text{III}}] > 1. \quad (25)$$

This modified barrier has two effects on the bubble size distribution. Unlike for a single type of ionizing sources, the left-hand side need not be a monotonically increasing function of

the overdensity δ . Its derivative vanishes when

$$p_{\text{II}} + \frac{f_{\text{coll}}}{f'_{\text{coll}}} p'_{\text{II}} = \frac{\zeta_{\text{III}}}{\zeta_{\text{III}} - \zeta_{\text{II}}}. \quad (26)$$

Physically, if $\zeta_{\text{III}} \gg \zeta_{\text{II}}$ and if high-density regions have enriched themselves, then it is possible for these regions to remain neutral even though regions with slightly smaller densities (and thus incomplete enrichment) can self-ionize.

As an example, we consider the choice $p_{\text{II}} = 1 - \exp(-\xi f_{\text{coll}})$, which essentially reflects the wind model from §3 (ignoring f_{new}). Here the enrichment probability is a function of density through its dependence on the collapse fraction; the exponential accounts for overlap of bubbles from randomly distributed sources within each region. Equation (26) then implies that the ionizing efficiency turns over at $\xi f_{\text{coll}} \approx 0.8$ for $\zeta_{\text{III}} \gg \zeta_{\text{II}}$, and some regions sufficiently far above this threshold could remain neutral.⁴ Note that not every region with $\xi f_{\text{coll}} > 0.8$ would be neutral; above this point, the effective ζ decreases with increasing δ but not necessarily by enough to become neutral. Moreover, a dense region could still be ionized by its neighbors (Barkana & Loeb 2004). The turnover with density can mimic “outside-in” reionization in which voids are ionized before intergalactic sheets and filaments (where the sources are located). However, for this effect to be significant we must have $\xi f_{\text{coll}}(\delta = 0) \approx 0.8$; this only occurs when enrichment nears completion, well after reionization is complete in most cases. Thus in this simple, wind-driven model we do not expect neutral dense regions to be common during reionization.

Unfortunately, once the ionizing efficiency turns over, the excursion set formalism of FZH04 breaks down. This is because the number of ionizing photons is no longer additive in a simple way, but rather depends on the degree of enrichment of substructure inside the region of interest. However, if $\xi f_{\text{coll}}(\delta = 0)$ remains reasonably small during reionization then the model can still be used. In this limit, we consider how the shape of the barrier – and hence the shape of the bubble size distribution – changes due to the metal enrichment pattern. In standard reionization scenarios, the shape is set by $f_{\text{coll}} = \text{constant}$ (the solution to $\zeta f_{\text{coll}} = 1$). With enrichment, equation (25) shows that the shape is instead set by a condition on a combination of f_{coll} and p_{II} . Unfortunately, the dependence is weak for reasonable choices of p_{II} . For example, with the simple wind model examined above, p_{II} is purely a function of f_{coll} and the shape is still determined by $f_{\text{coll}} = \text{constant}$; it can be exactly reproduced by choosing an effective ζ_{eff} to match the total ionized fraction.

Thus, to change the shape, p_{II} must have a more complicated density dependence. Let us consider the simple parameterization

$$p_{\text{II}} = 1 - \exp \left[-\xi f_{\text{coll}} \left(1 + A \frac{|\delta|}{1+z} \right) \right], \quad (27)$$

where A is some constant that measures the steepness of the density dependence. This form has the limits $p_{\text{II}} \rightarrow 1$ for $\delta \rightarrow \infty$ and $p_{\text{II}} \rightarrow 0$ for $\delta \rightarrow -\infty$, and it concentrates enrichment in dense regions more than the simple wind model does. One reason this may happen is that $f_{\text{new}}/f_{\text{coll}}$ is smaller than the average in dense regions because they are further along in the structure formation process. Qualitatively, we expect

⁴ Note that f_{coll} actually depends on the scale of interest (as could p_{II}). We neglect this here, considering only those scales for which $\sigma_{\text{min}} \gg \sigma(m)$.

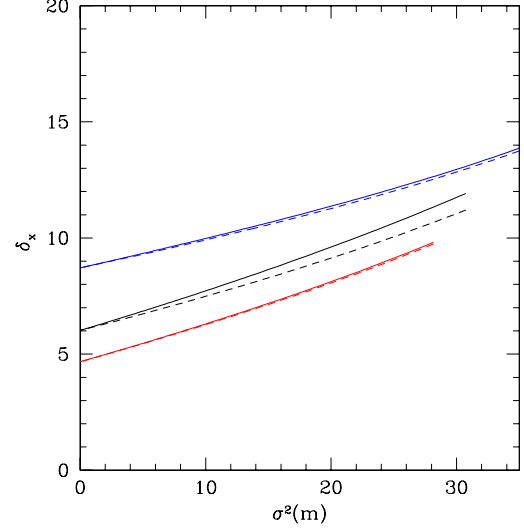


FIG. 8.— Sample barriers from equation (27) (solid curves) and for a single type of source (dashed curves) with the same limiting value at $\sigma^2 = 0$. In each case, $\zeta_{\text{III}} = 44$, $\zeta_{\text{II}} = 9$, and $A = 1$. We show results for $\xi = 5, 15$, and 25 , from bottom to top.

the barrier to be somewhat steeper with this prescription, because dense regions have extra enrichment and fewer ionizing photons. The solid curves in Figure 8 show some example barriers. In each case, $\zeta_{\text{III}} = 44$, $\zeta_{\text{II}} = 9$, and $A = 1$. We show $\xi = 5, 15$, and 25 , from bottom to top. The dashed curves show the barrier for a single source type with the value at $\sigma^2 = 0$ fixed to match the solid curves. These have $\zeta_{\text{eff}} = 38, 24$, and 11 for the three values of ξ . Indeed the barriers are steeper, which implies fewer small bubbles because small, dense clusters are highly enriched. However, we find that the steepening is relatively weak, especially when one of the two star formation modes dominates (i.e., $\zeta_{\text{eff}} \approx \zeta_{\text{III}}$ or ζ_{II}). Of course, if enrichment is sufficiently extensive that equation (26) is violated, the barrier approach breaks down and the bubble pattern could change significantly.

We have considered other possible parameterizations of p_{II} based around the simple wind expression; in the cases we examined, the differences were not much larger than shown in Figure 8. The reason is that p_{II} is simply used to interpolate between two different populations, each of which would follow the usual barrier. In addition, the interpolation between them also depends on the collapse fraction. Thus it appears difficult to change the shape dramatically, although exotic scenarios in which the collapse fraction played no role could have stronger effects.

7. DISCUSSION

We have examined a variety of feedback mechanisms that could potentially yield “double reionization,” for which the globally-averaged ionized fraction \bar{x}_i decreases over a limited period of cosmic time. These mechanisms include metal enrichment, photoionization heating, and photodissociation of H_2 . We constructed simple models that nevertheless retained the crucial physics; as a result we were able to vary a relatively small set of parameters to pin down the requirements for double reionization. In all cases, we found that double reionization requires unusual (though not impossible) parameter choices. In particular, it requires a rapid drop in the ionizing emissivity over a single recombination time (see equa-

tion [18]). Because the recombination time varies spatially within the IGM, we found that it is not difficult to imagine relatively dense pockets recombining after feedback becomes strong (which could affect the topology of ionized gas; see §6), but because the majority of the universe lies near the cosmic mean density, global double reionization will be difficult to arrange.

For metal enrichment, we require three conditions: (i) $\zeta_{\text{III}}/\zeta_{\text{II}} \gg 1$, (ii) an average clumping factor much larger than unity, and (iii) winds that expand much more rapidly than predicted by existing semi-analytic models (Madau et al. 2001; Scannapieco et al. 2002; Furlanetto & Loeb 2003). We have argued that condition (ii) is implausible for the majority of the IGM (Miralda-Escudé et al. 2000) and that (iii) is similarly implausible, so we regard this mechanism as unlikely to cause double reionization. Although quasar winds could significantly hasten the enrichment if the star formation efficiency is low in small halos, they are not sufficiently powerful to alter this conclusion. Existing work predicted double reionization only because of an artificial, instantaneous transition between star-forming modes (Wyithe & Loeb 2003a; Cen 2003a; see also Haiman & Holder 2003). Our models are more similar to Scannapieco et al. (2003), who found a gradual disappearance of Pop III stars. In a hierarchical picture, the decline has two causes: (i) accretion shifts to higher mass, pre-enriched halos, and (ii) the slow expansion of galactic winds. The first depends on unknown halo merger rates, but our estimate appears to be conservative. Interestingly, when we normalize the wind sizes to semi-analytic models, our results imply incomplete enrichment at $z \sim 6$, suggesting that Pop III stars may be observable in the foreseeable future (see also Scannapieco et al. 2003).

Double reionization from photoionization heating is more plausible. In this case we require that (i) $T_h/T_c \gg 1$ and (ii) small halos (those with $T_{\text{vir}} < T_h$) contribute a large fraction of the ionizing photons. The latter implies that the star formation efficiency does not drop too rapidly with decreasing halo mass. In particular, if $f_* \propto m^{2/3}$ persists at high redshifts (as has been observed in nearby galaxies; Dekel & Woo 2003; Kauffmann et al. 2003), then small halos do not dominate the ionizing photon budget and double reionization cannot occur. Quasars also help to wash out double reionization if the black hole mass scales steeply with host halo mass, as in Wyithe & Loeb (2003c). We argued that the photoheating occurs more rapidly than ionization, because photons are preferentially emitted in regions that have remained neutral to that point, while recombinations are confined to ionized regions. Thus double reionization from this mechanism always begins before $\bar{x}_i = 1$. Our fiducial choice of $T_h/T_c = 25$ is on the threshold of double reionization; if photoheating is less efficient at suppressing galaxy formation near the time of recombination (Dijkstra et al. 2004a), then this mechanism cannot cause double reionization. Note also that, if the first sources produce X-ray photons (e.g. Ricotti et al. 2004; but see Dijkstra et al. 2004b), the IGM will be heated gradually and (nearly) uniformly, again suppressing accretion onto small halos (Oh & Haiman 2003). This would tend to smooth out the transition from T_c to T_h , decreasing the likelihood of double reionization.

Finally, H_2 photodissociation has a similar phenomenolog-

ical effect to photoheating, increasing the minimum mass for star formation (albeit from a much lower base level). However, we showed that the feedback threshold must be reached when the ionized fraction is still small, so the recombination phase would be difficult to observe. Haiman et al. (2000) also reached this conclusion through more detailed modeling.

We have not examined any combinations of these different mechanisms. Together they could increase the contrast between the initial and final ionizing efficiency, which would make double reionization somewhat easier to achieve. For example, photoionization heating could extend reionization over a long interval. This would increase the time over which winds can expand and hence move the Pop III/II transition closer to reionization, increasing the effective amount of suppression in ionized regions. Another possibility is that star formation through H_2 cooling at extremely high redshifts could begin to spread metals throughout the IGM. Once photodissociation dominates, there would be a long pause until reionization could continue. Again, the winds would have extra time to expand. However, given the small scales that we have estimated for the wind regions during reionization, these processes are unlikely to change our qualitative conclusions.

We have focused here on particular ionization histories in which \bar{x}_i turns over. We found that such scenarios are difficult to achieve. But we stress that *extended* reionization is not nearly so difficult; any form of feedback will help to prolong the reionization era and to relieve the apparent tension between the $z \sim 6$ quasar data (Fan et al. 2002; Wyithe & Loeb 2004a; Mesinger & Haiman 2004) and the optical depth to electron scattering measured by *WMAP* (Kogut et al. 2003). Moreover, we have found that a turnover in the emissivity is also not difficult to achieve; all of our feedback scenarios yield this kind of behavior, at least if low-mass halos have high star formation efficiencies. Unfortunately, the emissivity evolution is harder to measure.

Finally, we must also stress that we have studied double reionization in a *global* sense. Although we have found that \bar{x}_i only turns over in exceptional circumstances, the reionization history of any particular region or line of sight need not be monotonic. For example, if photoheating suppression is important, a volume ionized early on will experience a sharp decrease in its emissivity and begin to recombine. Only later will halos grow sufficiently massive to ionize it again. Our models show that, while this region is recombining, others are also being ionized and that these often dominate the global evolution. The most promising way to probe reionization in different physical volumes is 21 cm tomography (Madau et al. 1997; Zaldarriaga et al. 2004; Furlanetto et al. 2004c). We have argued that these feedback mechanisms should induce signatures in the bubble size distribution, although the metal enrichment appears to have little effect except in dense, highly-enriched regions. Because of the complexity of this problem, numerical simulations would provide the best method to examine changes in the bubble pattern in greater detail.

We thank M. Kamionkowski for helpful discussions. This work was supported in part by NSF grants AST-0204514, AST-0071019 and NASA grant NAG 5-13292 (for A.L.).

REFERENCES

Abel, T., Bryan, G. L., & Norman, M. L. 2002, *Science*, 295, 93
Aguirre, A., et al. 2001, *ApJ*, 561, 521

Barkana, R., & Loeb, A. 1999, *ApJ*, 523, 54
—. 2001, *Phys. Rep.*, 349, 125

—. 2004, *ApJ*, 609, 474

Becker, R. H., et al. 2001, *AJ*, 122, 2850

Benson, A. J., Kamionkowski, M., & Hassan, S. H. 2004, *MNRAS*, submitted (astro-ph/00407136)

Bond, J. R., Cole, S., Efstathiou, G., & Kaiser, N. 1991, *ApJ*, 379, 440

Bromm, V., Coppi, P. S., & Larson, R. B. 2002, *ApJ*, 564, 23

Bromm, V., Ferrara, A., Coppi, P. S., & Larson, R. B. 2001a, *MNRAS*, 328, 969

Bromm, V., Kudritzki, R. P., & Loeb, A. 2001b, *ApJ*, 552, 464

Bromm, V., & Loeb, A. 2003, *Nature*, 425, 812

Cen, R. 2003a, *ApJ*, 591, L5

—. 2003b, *ApJ*, 591, 12

—. 2003c, *ApJ*, submitted (astro-ph/0311329)

Ciardi, B., & Madau, P. 2003, *ApJ*, 596, 1

Cole, S., Aragon-Salamanca, A., Frenk, C. S., Navarro, J. F., & Zepf, S. E. 1994, *MNRAS*, 271, 781

Dekel, A., & Woo, J. 2003, *MNRAS*, 344, 1131

Dijkstra, M., Haiman, Z., Rees, M. J., & Weinberg, D. H. 2004, *ApJ*, 601, 666

Dijkstra, M., Haiman, Z., Loeb, A. 2004, *ApJ*, in press (astro-ph/040307)

Efstathiou, G. 1992, *MNRAS*, 256, 43

Fan, X., et al. 2002, *AJ*, 123, 1247

Fukugita, M., & Kawasaki, M. 2003, *MNRAS*, 343, L25

Furlanetto, S. R., Hernquist, L., & Zaldarriaga, M. 2004a, *MNRAS*, in press (astro-ph/0406131)

Furlanetto, S. R., & Loeb, A. 2001, *ApJ*, 556, 619

—. 2003, *ApJ*, 588, 18

Furlanetto, S. R., Zaldarriaga, M., & Hernquist, L. 2004b, *ApJ*, 613, 1 [FZH04]

—. 2004c, *ApJ*, 613, 16

Gnedin, N. Y. & Hui, L. 1998, *MNRAS*, 296, 44

Gunn, J. E., & Peterson, B. A. 1965, *ApJ*, 142, 1633

Haiman, Z., Thoul, A. A., & Loeb, A. 1996, *ApJ*, 464, 523

Haiman, Z., Abel, T., & Madau, P. 2001, *ApJ*, 551, 599

Haiman, Z., Abel, T., & Rees, M. J. 2000, *ApJ*, 534, 11

Haiman, Z., & Holder, G. P. 2003, *ApJ*, 595, 1

Haiman, Z., Rees, M. J., & Loeb, A. 1997, *ApJ*, 476, 458; 484, 985

Heger, A., & Woosley, S. E. 2002, *ApJ*, 567, 532

Hui, L., & Haiman, Z. 2003, *ApJ*, 596, 9

Kauffmann, G., & White, S. D. M. 1993, *MNRAS*, 261, 921

Kauffmann, G., et al. 2003, *MNRAS*, 341, 54

Kitayama, T., & Ikeuchi, S. 2000, *ApJ*, 529, 615

Kogut, A., et al. 2003, *ApJS*, 148, 161

Lacey, C., & Cole, S. 1993, *MNRAS*, 262, 627

Machacek, M. E., Bryan, G. L., & Abel, T. 2001, *ApJ*, 548, 509

Madau, P., Ferrara, A., & Rees, M. J. 2001, *ApJ*, 555, 92

Madau, P., Meiksin, A., & Rees, M. J. 1997, *ApJ*, 475, 429

Mesinger, A., & Haiman, Z. 2004, *ApJ*, 611, L69

Miralda-Escudé, J., Haehnelt, M., & Rees, M. J. 2000, *ApJ*, 530, 1

Mo, H. J., & White, S. D. M. 1996, *MNRAS*, 282, 347

Mori, M., Ferrara, A., & Madau, P. 2002, *ApJ*, 571, 40

Oh, S. P., & Haiman, Z. 2003, *MNRAS*, 346, 456

Onken, C. A., & Miralda-Escudé, J. 2004, *ApJ*, 610, 1

Press, W. H., & Schechter, P. 1974, *ApJ*, 187, 425

Rees, M. J. 1986, *MNRAS*, 222, 27P

Ricotti, M., Gnedin, N. Y., & Shull, J. M. 2002, *ApJ*, 575, 49

Ricotti, M., Gnedin, N. Y., & Ostriker, J. P. 2004, *ApJ*, submitted (astro-ph/0404318)

Sasaki, S. 1994, *PASJ*, 46, 427

Scalo, J. 1998, in *ASP Conf. Ser.* 142: The Stellar Initial Mass Function, ed. G. Gilmore and D. Howell (San Francisco: ASP), 201

Scannapieco, E., Thacker, R. J., & Davis, M. 2001, *ApJ*, 557, 605

Scannapieco, E. & Barkana, R. 2002, *ApJ*, 571, 585

Scannapieco, E., Ferrara, A., & Madau, P. 2002, *ApJ*, 574, 590

Scannapieco, E., Schneider, R., & Ferrara, A. 2003, *ApJ*, 589, 35

Sedov, L. I. 1959, *Similarity and Dimensional Methods in Mechanics* (New York: Academic Press)

Shapiro, P. R., & Giroux, M. L. 1987, *ApJ*, 321, L107

Shapiro, P. R., Iliev, I. T., & Raga, A. C. 2004, *MNRAS*, 348, 753

Sheth, R. K. 1998, *MNRAS*, 300, 1057

Sokasian, A., et al. 2004, *MNRAS*, 350, 47

Somerville, R. S., & Kolatt, T. S. 1999, *MNRAS*, 305, 1

Somerville, R. S., & Livio, M. 2003, *ApJ*, 593, 611

Songaila, A. 2004, *AJ*, 127, 2598

Spergel, D. N., et al. 2003, *ApJS*, 148, 175

Strickland, D. K., Heckman, T. M., Weaver, K. A., & Dahlem, M. 2000, *AJ*, 120, 2965

Tegmark, M., et al. 1997, *ApJ*, 474, 1

Theuns, T., et al. 2002, *ApJ*, 567, L103

Thoul, A. A., & Weinberg, D. H. 1996, *ApJ*, 465, 608

Verde, L., Kamionkowski, M., Mohr, J. J., & Benson, A. J. 2001, *MNRAS*, 321, L7

Whalen, D., Abel, T., & Norman, M. L. 2004, *ApJ*, 610, 14

White, R. L., Becker, R. H., Fan, X., & Strauss, M. A. 2003, *AJ*, 126, 1

Wyithe, J. S. B., & Loeb, A. 2002, *ApJ*, 581, 886

—. 2003a, *ApJ*, 586, 693

—. 2003b, *ApJ*, 588, L69

—. 2003c, *ApJ*, 595, 614

—. 2004a, *Nature*, 427, 815

—. 2004b, *ApJ*, submitted (astro-ph/0407162)

—. 2004c, *Nature*, in press (astro-ph/0409412)

Zaldarriaga, M., Furlanetto, S. R., & Hernquist, L. 2004, *ApJ*, 608, 622